# Journal of Materials Chemistry B

Accepted Manuscript






ROYAL SOCIETY OF CHEMISTRY

www.rsc.org/materialsB

Cite this: DOI: 10.1039/c0xx00000x

www.rsc.org/xxxxxx

ARTICLE TYPE

# Hollow hierarchical hydroxyapatite/Au/polyelectrolyte hybrid microparticles for multi-responsive drug delivery

**Shuhan Xu, Jun Shi*, Desheng Feng, Liu Yang and Shaokui Cao***

***Received (in XXX, XXX) Xth XXXXXXXXX 20XX, Accepted Xth XXXXXXXXX 20XX***
**DOI: 10.1039/b000000x**

In this work, hollow hierarchical hydroxyapatite (HAP)/Au/polyelectrolyte hybrid microparticles with a hollow HAP core and polymer multilayer/Au nanoparticles (AuNPs) shell for multi-responsive drug delivery have been prepared via layer-by-layer (LbL) technique. Thermal-/pH- dual responsive aliphatic poly(urethane-amine) (PUA) was employed as the smart component. The aggregated AuNPs inside hybrid microparticles could potentially obstruct the diffusion of doxorubicin hydrochloride (DOX) from the hollow microparticles and assuage the initial burst release of DOX. Upon irradiation with near-infrared (NIR) laser, AuNPs aggregates can effectively convert light to heat and result in the rapid release of DOX due to the partial collapse of the polyelectrolyte multilayers (PUA/sodium poly(styrenesulfonate) (PSS)). In addition, thanks to the dissolution of HAP in the acidic media and the shrinkage of aliphatic PUA above its lower critical solution temperature (LCST), the drug release of hollow hybrid carriers exhibit distinuished pH- and thermal-dependent property. The results indicate that the hollow HAP/Au/PUA/PSS hybrid microparticles show great potential as a novel smart drug carrier for the controllable drug delivery.

***Keywords:*** hydroxyapatite, self-assembly, hollow, multi-responsive drug delivery, near-infrared

## 1. Introduction

Stimuli-responsive hollow micro- and nano-capsules have recently attracted increasing attention, due to their potential applications as novel functional drug carriers.[1-4] However, a majority of them deal with the response to a single stimulus. In nature, the change in behavior of a macromolecule (proteins and nucleic acids) is often the combination of multi-environmental changes (such as temperature, pH value and magnetic fields), rather than a single factor. Compared with single responsive capsules, nano/micro drug carriers that can respond to more than one stimulus are very interesting owing to their physiological and biological applications.[5-7] Therefore, formulation of materials which can respond to multiple stimuli in a predictable manner would be of great interest. At present, there are some reports concerning the preparation of the multi-responsive micro/nano capsules for smart drug release. For example, Wang et al. synthesized multi-responsive polymeric nanocarriers based on the amphiphilic block copolymer for controlled release of bioactive agents.[8] Wu et al. prepared multi-responsive nitrobenzene-based amphiphilic copolymer assemblies for controlled release of Nile Red.[9] However, most of them is derived from the polymeric nanogels, which would require complicated synthesis route and introduce harmful chemical reagent to the resulting drug carriers.[8-11] Therefore, it is a great challenge to obtain multi-responsive drug carriers via simple and environmentally friendly method.

As a major inorganic constituent of teeth and bones, hydroxyapatite ($Ca_{10}(PO_4)_6(OH)_2$, HAP) has been widely used in biomedical area because of its good biological activity, biocompatibility and biodegradability.[12-14] In recent years, a number of studies have been carried out to investigate various HAP-based drug carriers. Among different morphological and structural HAP biomaterials, hollow HAP microparticles with high specific surface area and high capacity for drug loading show great potential as the novel drug carriers.[15,16] However, a rapid initial burst release is observed when HAP hollow microparticles are used as the drug delivery vehicles, which will limit the broad applications of hollow HAP microparticles in drug delivery area.[17-19]

In the present paper, H-HAP/Au/polyelectrolyte (H-HAP refers to hollow HAP) hybrid microparticles with near-infrared (NIR), pH and temperature triple-responsive drug delivery properties have been prepared via facile layer-by-layer method. The ability to remotely release the encapsulated materials at the specified location is very important in drug delivery area.[20-22] Au nanoparticle aggregates (AuNPs), which could absorb NIR light and then realize NIR photothermal ablation, have been widely employed in thermotherapy by local laser irradiation.[23-25] As illustrated in Scheme 1, HAP was fabricated by hydrothermal method using vaterite $CaCO_3$ as template. HAP microparticles could easily incorporate with polyelectrolytes (aliphatic

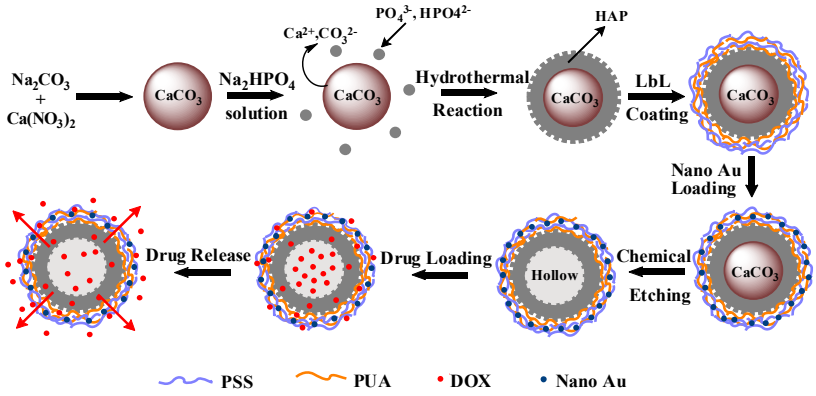


**Scheme 1.** Schematic illustration of the fabrication of H-HAP/Au/PUA/PSS hybrid microparticles.

poly(urethane-amine) (PUA) and sodium poly(styrenesulfonate) (PSS)) via layer-by-layer (LbL) technique. Then, AuNPs aggregates were loaded into the hybrid microparticles via electrostatic interaction. Finally, H-HAP/Au/PUA/PSS hybrid microparticles with a hollow HAP core and polymer multilayer/ AuNPs shell have were easily obtained by removing the $CaCO_3$ cores with acetic acid as illustrated in Scheme 2.

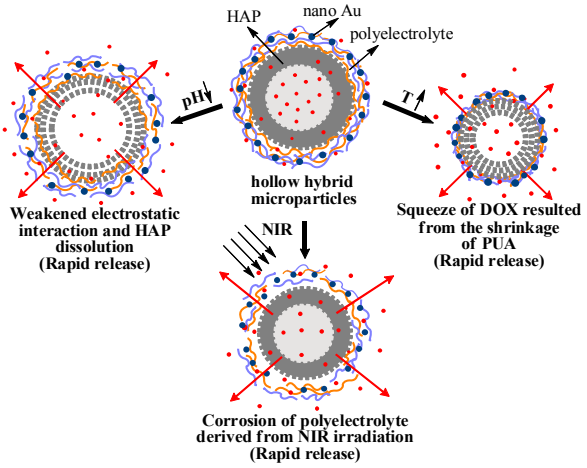


**Scheme 2**. Schematic illustration of triple-responsive (near-infrared/pH/ temperature) drug delivery from H-HAP/Au/PUA/PSS hybrid microparticles.

Thermal-/pH- dual responsive aliphatic PUA was employed as the smart component in this paper. Aliphatic PUA has attracted much attention in biological area, because of its thermally induced reversible transition property in aqueous solution at its LCST.[26,27] Moreover, the amine group of aliphatic PUA would change to the protonated amino forms with the decrease of pH value. Therefore, aliphatic PUA shows distinct pH- and thermal-dual responsive property, which has attracted a great deal of interest for potential applications in smart drug delivery.[28-30] Loaded AuNPs aggregates endow the hybrid microparticles with the NIR-responsive drug release property. In addition, AuNPs aggregates inside hybrid particles could potentially hinder DOX escaping from the hollow microparticles and assuage the initial burst release of DOX. More importantly, thanks to the dissolution of HAP in the acidic media and the shrinkage of aliphatic PUA above its LCST, the drug release of prepared hollow carriers exhibited distinguished pH- and thermal-dependent property as illustrated in Scheme 2. The present paper provides a facile and green route to fabricate smart hierarchical hybrid hollow drug carrier by combining polyelectrolytes, inorganic microparticles and metal nanoparticles, which is highly attractive for drug delivery system.

## 2. Experimental section

### 2.1 Materials

Sodium poly(styrenesulfonate) (PSS, $M_w$ = 70000, Alfa Organics, China), doxorubicin hydrochloride (DOX, Beijing Huafenglianbo Chemical, China), calcium nitrate ($Ca(NO_3)_2$, Tianjin Chemical Reagent Factory, China), disodium hydrogen phosphate dodecahydrate ($Na_2HPO_4 \cdot 12H_2O$, Tianjin Dengke Chemical, China), sodium carbonate ($Na_2CO_3$, Tianjin Hengxing Chemical, China) and chloroauric acid tetrahydrate ($HAuCl_4 \cdot 4H_2O$, Sinopharm Chemical Reagent Co., China) were analytical reagents and used as received. The aliphatic PUA was synthesized by the copolymerization of 2-methylaziridine with $CO_2$ according to literature.[27] The LCST of aliphatic PUA is 50 $^oC$ as measured by a temperature-variable UV-vis spectrometer (see Fig. S1). The urethane content calculated from elemental analyses is 41.86 %. $M_w$ and PDI of the aliphatic PUA are $1.2\times10^4$ and 1.67, respectively.

### 2.2 Preparation of HAP microparticles with a $CaCO_3$ core

$Na_2CO_3$ solution (0.1 M, 20 mL) was rapidly poured into $Ca(NO_3)_2$ (0.1 M, 20 mL) and PSS (10 mg/mL) mixed solution under magnetic agitation. The solution was kept at 30 $^oC$ for 30 min. The vaterite microparticles were washed with distilled water for three times and then collected by centrifugation. The vaterite $CaCO_3$ were mixed with $Na_2HPO_4$ solution (0.93 M, 30 mL). The suspension was transferred into 100 mL of autoclave, sealed, and heated by hydrothermal method at 140 $^oC$ for 4 h. The product was washed with distilled water for three times and then collected by centrifugation.

### 2.3 Preparation of Au nanoparticles

AuNPs were synthesized according to Frens' method with minor modification. Typically, 0.2 ml of sodium citrate (0.189 M) was added to 20 ml of boiling $HAuCl_4$ solution (0.25 mM). After 15 min boiling, the heat source was removed. The colloid

solution was further stirred for 15 min and then stored in the dark at 4 °C.

### 2.4 Preparation of H-HAP/Au/PUA/PSS hybrid microparticles

HAP with a $CaCO_3$ core was used as the template to fabricate H-HAP/Au/PUA/PSS hybrid microparticles via LbL technique. Typically, HAP was incubated in 8 mL of PUA /NaCl solution (2 mg/mL, pH 6.0) for 10 min followed by a centrifugation/washing procedure for 3 times. Then the microparticles were incubated in 8 mL of PSS/NaCl solution (2 mg/mL, pH 6.0) for 10 min followed by a centrifugation/washing procedure for 3 times. To form AuNPs aggregates, 2 mL of NaCl (0.5 M) and AuNPs solution were mixed for 2 min. After self-assembly of five layers of polyelectrolytes, AuNPs agglomerates were deposited on HAP via electrostatic interaction. Three washing steps followed the AuNPs deposition and one more layer of PSS was then added. Finally, $(PUA/PSS)_3$ multilayers and one layer of AuNPs agglomerates were deposited on HAP microparticles. By removing the $CaCO_3$ cores with 0.1 M of acetic acid (pH 4.5), H-HAP/Au/PUA/PSS hybrid microparticles were finally obtained. The resulting hollow hybrid microparticles consisted of HAP with three bilayers of polyelectrolyte embedded with AuNPs aggregates. As a control test, pure HAP and hollow HAP/polyelectrolyte hybrid microparticles without AuNPs (H-HAP/PUA/PSS) were prepared with the aforementioned scheme.

### 2.5 Characterization of H-HAP/Au/PUA/PSS hybrid microparticles

The high magnification morphology was observed using a field emission scanning electron microscopy (FESEM, JEOL 7500F). Before observation, the particles were coated with an approximate 100 Å layer of platinum. FT-IR spectra were recorded with a Nicolet Protégé 460 FT-IR spectrometer in the range of 4000-500 $cm^{-1}$ using KBr pellets. The formation of HAP and the incorporation of AuNPs were confirmed by means of energy dispersive X-ray spectrometer (EDX, INCA). Transmission electron microscopy (TEM) were carried out on Tecnai G2 20 emission electron microscope (FEI) using the copper grid as the sample holder operated at 200 kV. Zeta-potential of the particles during the LbL process was measured in 0.025 M of NaCl solution with a pH value of 6.0 by a Zeta-sizer (nano ZS90 Malvern Instruments). At least three measurements were performed for each sample and the average values are shown as resulting zeta-potential. X-ray diffraction (XRD) patterns were recorded on a Bruker D8 Advance diffractometer using Cu-Ka radiation (λ= 1.54178 Å) with a graphite monochromator.Thermogravimetric analysis (TGA) was taken on a TGA/DSC Simultaneous Thermogravimetric Analyzer (Netzsch STA449 F3) with the heating rate of 10 °C $min^{-1}$ under Ar atmosphere.

### 2.6 Determination of drug encapsulation efficiency and in vitro release studies

50 mg of sample was transferred into DOX (0.5 $mg{\cdot}mL^{-1}$)/NaCl solution for 12 h under gentle shaking at 30 °C. Then, DOX-loaded microparticles were obtained by washing with water for 3 times and collected by centrifugation and then vacuum dried at 40 °C for 24 h. The DOX amounts of the clear supernatant were measured by UV-vis absorption spectroscopy at 481 nm and calculated by employing a calibration curve. Taking away the clear supernatant DOX content from the feed drug content, the loading DOX content in microcapsules would be calculated. The loading efficiency is defined as the weight percentage of loaded drug based on feed amount.

For in vitro drug release test, the DOX-loaded microparticles (10 mg) were suspended in 30 mL of release medium with different pH values and temperatures. The sample (3 mL) was periodically removed and the withdrawn sample was replaced by the same volume of fresh medium. For the NIR laser experiments, 3 mg of microparticles were suspended in 1 mL of PBS solution at room temperature. A continuous wave (CW) laser source (780 nm, 120 mw) was employed and the samples were irradiated repeatedly over a period of 15 min, followed by 45 min intervals with the laser turned off. The sample (0.1 mL) was periodically removed and then diluted to 2 mL and the withdrawn sample was replaced by the same volume of fresh medium. The amount of released drug was analysed with a UV spectrophotometer. All the tests were carried out in triplicate and the average values were shown in this study.

## 3. Results and Discussion

### 3.1 Aggregation of Au nanoparticles

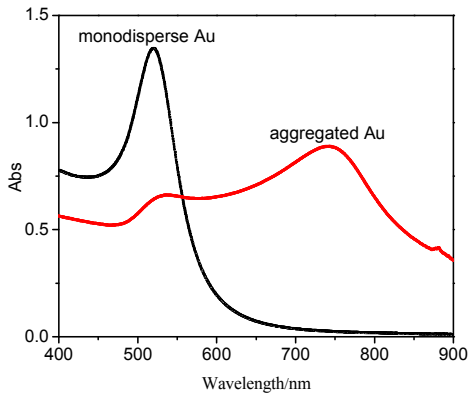


**Fig. 1.** UV-Vis-NIR extinction spectra of monodisperse AuNPs and AuNPs aggregates (by adding 0.5 M of NaCl solutions for 2 min).

AuNPs agglomerates can be generated by adding NaCl solutions to the monodisperse AuNPs solutions. NaCl increased the ionic strength of AuNPs solutions, which could weaken the repulsion between the functional groups of AuNPs and then accelerate the accumulation of AuNPs.[23,24] The typical UV-Vis-NIR extinction spectra of monodisperse AuNPs and AuNPs aggregates (by adding 0.5 M of NaCl solutions for 2 min) were shown in Fig. 1. After aggregation, AuNPs solutions became unstable and the solution rapidly changed from red to blue/grey. The corresponding absorption spectrum displays a new broad absorption region between 700 and 900 nm with a maximum absorption peak at 743 nm, indicating the good absorption ability of AuNPs agglomerates at NIR area.[21,22]

### 3.2 Characterization of H-HAP/Au/PUA/PSS hybrid microparticles

In the present work, PSS–doped HAP has been fabricated by hydrothermal method using PSS–doped vaterite $CaCO_3$ as

template and $Ca^{2+}$ source. PSS has been used as crystal growth additive to accelerate the transformation of $CaCO_3$ from calcite to vaterite during the course of $CaCO_3$ preparation.[28,29] In addition, negatively charged PSS would improve the bonding force between HAP microparticles and polyelectrolytes. In order to study the multi-responsive release property of H-HAP/Au/PUA/PSS hybrid microparticles, three samples have been prepared as illustrated in Table 1: solid HAP, H-HAP/PUA/PSS and H-HAP/Au/PUA/PSS hybrid microparticles (H-HAP refers to HAP hollow microparticles).

**Table 1** Composition and drug loading efficiency of the samples

| Sample | Compositions | Drug content (mg/per 10mg sample) | Loading efficiency (%) |
|---|---|---|---|
| 1 | Solid HAP | 0.158 ± 0.007 | 39.6 ± 1.7 |
| 2 | H-HAP/PUA/PSS | 0.433 ± 0.032 | 69.4 ± 2.0 |
| 3 | H-HAP/Au/PUA/PSS | 0.374 ± 0.034 | 58.6 ± 1.9 |

Fig. 2 shows TEM images of AuNPs and H-HAP/Au/PUA/PSS hybrid microparticles. As shown by Fig. 2A, the monodisperse AuNPs are spherical in shape with an average diameter of 20 nm. According to Fig. 2B, the typical TEM image of HAP solid microparticles had a black centre, indicating the presence of a solid $CaCO_3$ core. However, the disappearance of the black centre in Fig. 2C suggested the hollow structure of the H-HAP/Au/PUA/PSS hybrid microparticles.[19] In addition, AuNPs aggregates could be clearly observed around the surface of hollow hybrid microparticles and the wall thickness is about 0.6 μm. Comparing the high magnification TEM image of H-HAP/Au/PUA/PSS hybrid microparticles (Fig. 2E) with that of HAP microparticles (Fig. 2D), it could be observed that the HAP nanoneedles around the HAP microparticles were disappeared and the particle surface became smoother than that of HAP ones. The results demonstrate the successful adsorption of PUA/PSS multilayers around needle-like surface of HAP microparticles.

Fig. 3 shows FESEM micrographs and corresponding EDX spectra of the hybrid microparticles. PSS–doped $CaCO_3$ microparticles were spherical in shape with diameter of 1-2 μm (Fig. 3A). The size of HAP was slightly larger than that of $CaCO_3$ template (Fig. 3B) due to the formation of porous HAP nanoneedles deriving from hydrothermal process. The surface of HAP became more coarse and porous than that of $CaCO_3$ ones. The appearance of P elements in the EDX spectrum of HAP proved the formation of HAP (Fig. 3H). After assembly of $(PUA/PSS)_3$ multilayers and one layer of AuNPs agglomerates, the surfaces of multilayer-coated microparticles appeared more smooth than that of the uncoated ones (Fig. 3C), indicating the successful incorporation of PUA/PSS multilayers around the HAP. By removing the $CaCO_3$ core with acetic acid, H-HAP/Au/PUA/PSS hybrid microparticles were obtained (Fig. 3D). Partial structure collapse and capsule-like microparticles could be observed, which might be due to the oppression of PUA/PSS multilayers and AuNPs agglomerates on HAP hollow structures.[19,31] The corresponding EDX spectrum (Fig. 3I) confirmed the presence of N element coming from PUA and Au element deriving from AuNPs. The distinct P signal demonstrated that the HAP hollow structures could be successfully preserved after etching procedure. Comparing the high magnification FESEM image of H-HAP/Au/PUA/PSS hybrid microparticles before (Fig. 3E) and after NIR laser (Fig. 3F), it could be found that the nanoporous within the polyelectrolyte walls became slightly looser upon NIR laser irradiation.[32] This phenomenon may be ascribed to the photothermal effect of AuNPs agglomerates absorbing the laser light energy, which results in the partial collapse of PUA/PSS polyelectrolyte.

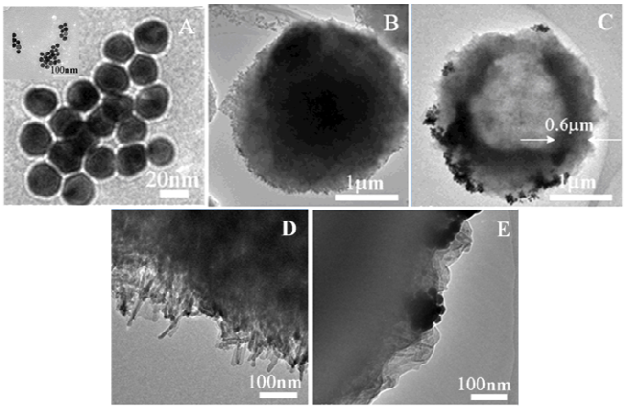


**Fig. 2.** TEM images of AuNPs (A), solid HAP (B), H-HAP/Au/PUA/PSS hybrid microparticles (C). The high magnification TEM images of solid HAP (D) and H-HAP/Au/PUA/PSS hybrid microparticles (E).

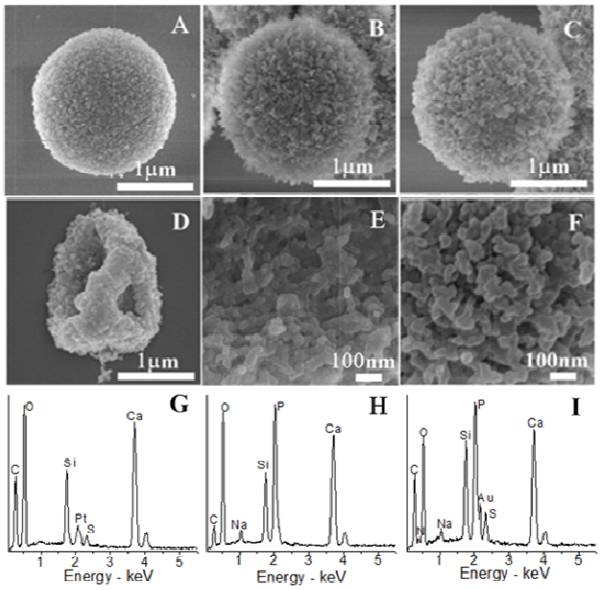


**Fig. 3.** FESEM micrographs and corresponding EDX spectra of vaterite $CaCO_3$ (A), HAP (B), HAP/Au/PUA/PSS hybrid microparticles (C) and H-HAP/Au/PUA/PSS hybrid microparticles (D). The high magnification of the surface of H-HAP/Au/PUA/PSS hollow hybrid microparticles before (E) and after (F) NIR laser irradiation. EDX spectra for vaterite $CaCO_3$ (G), HAP (H) and H-HAP/Au/PUA/PSS hollow hybrid microparticles (I).

Fig. 4A presents FT-IR spectra of HAP and H-HAP/Au/PUA/PSS hybrid microparticles. The characteristic bands at 1031, 603 and 564 $cm^{-1}$ were assigned to $PO_4^{3-}$ and the absorption peaks of B-type $CO_3^{2-}$ were located at 1459, 1413 and 874 $cm^{-1}$. Therefore, the absorption peaks corresponding to the functional groups of $CaCO_3$ core in HAP were overlapped by the

absorption peaks of B-type $CO_3^{2-}$. The absorbance of urethane groups in PUA at 1700, 1537 and 1217 $cm^{-1}$, the sulfonic groups in PSS at 1176 $cm^{-1}$, could be observed in the FT-IR spectrum of H-HAP/Au/PUA/PSS hybrid microparticles.[31,33] Fig. 4B presents the XRD patterns of HAP and H-HAP/Au/PUA/PSS hybrid microparticles. The phases including HAP and calcium carbonate were observed in HAP microparticles because a certain amount of calcium carbonate phases were remained in the HAP microparticles.[19] $CaCO_3$ core can be easily removed to produce HAP hollow microparticles because of the good solubility of $CaCO_3$ in acetic acid. Therefore, only HAP phase could be observed in the XRD patterns of H-HAP/Au/PUA/PSS hybrid microparticles. Au phase were also clearly observed in H-HAP/Au/PUA/PSS hybrid microparticles, indicating that AuNPs were successfully adsorbed into the polymer multilayers.

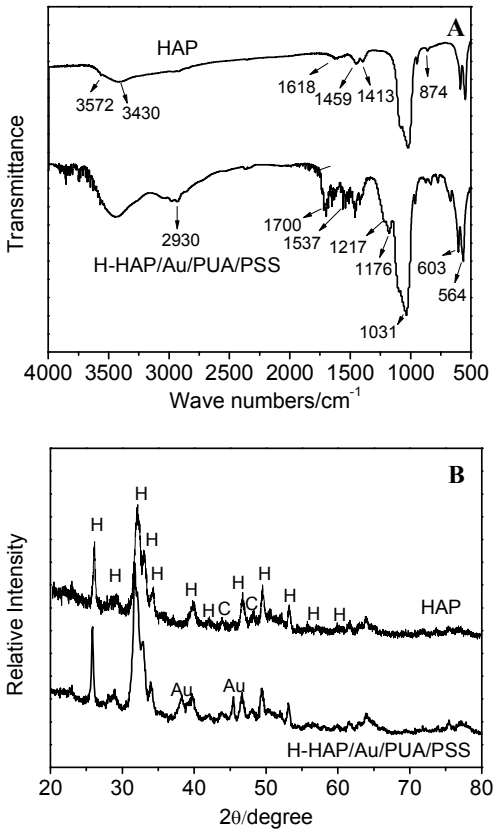


**Fig. 4.** FT-IR spectra (A) and XRD curves (B) for HAP and H-HAP/Au/PUA/PSS hybrid microparticles. "C" denotes for the $CaCO_3$ phase and "H" denotes for HAP phase.

The LbL self-assembly process was monitored by zeta-potential as shown in Fig. 5A. Since PSS is negatively charged, the zeta-potential of the PSS-doped $CaCO_3$ microparticles was around -17 mV. After hydrothermal reaction, the zeta-potential of the PSS-doped HAP microparticles changed to -23 mV. Partial of PSS inside $CaCO_3$ cores has transferred to the surface of HAP microparticles during the hydrothermal reaction process, resulting the increase of microparticle zeta-potential. Typical oscillations of the zeta-potential could be observed during the following LbL self-assembly process. It can be also noted that the zeta-potential is characterized by the overall negative zeta-potential throughout the entire multilayer formation due to the hydrogen bonding between the sulfonic groups of PSS and the urethane groups of PUA.[33,34] Fig. 5B shows the TG analysis curve of H-HAP/Au/PUA/PSS hybrid microparticles. In order to calculate the polymer content in H-HAP/Au/PUA/PSS hybrid microparticles, the TG analysis of HAP hollow microparticles was also presented in Fig. 5B. The weight loss of HAP hollow microparticles below 450 ºC (6.97%) was due to the adsorbed water and impurities hidden in the nanopores of HAP hollow microparticles.[19] The mass loss of 4.65% at 450-800 °C was ascribed to the decomposition of the B- and A-type carbonate ions. The weight loss of H-HAP/Au/PUA/PSS hybrid microparticles below 150 °C was due to the water evaporation. The weight loss of 16.78% at 150-450 °C corresponds to the decomposition of PUA/PSS multilayers, indicating that the polymer content in H-HAP/Au/PUA/PSS hybrid microparticles was around 16.78%. The mass loss at 450-800 °C corresponded to the decomposition of the B- and A-type carbonate ions.

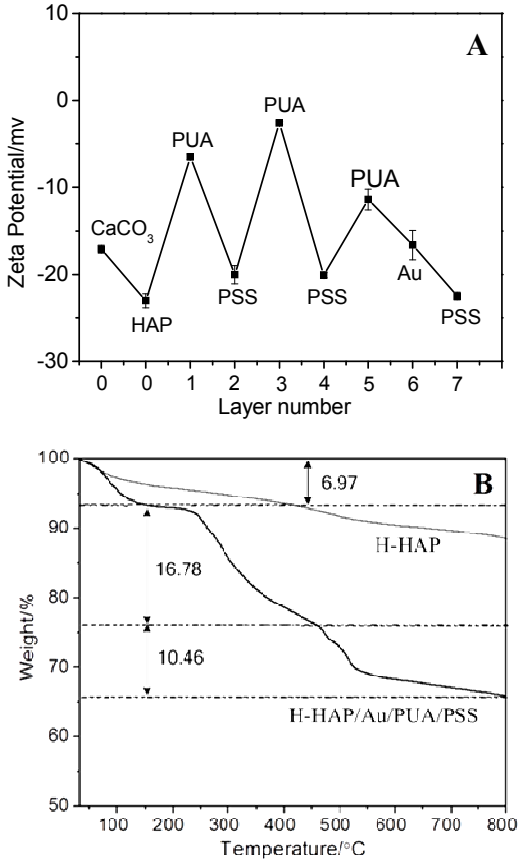


**Fig. 5.** Evolution of zeta-potential during deposition of $(PUA/PSS)_3$ multilayers on the surface of HAP (A) and TGA curves of HAP hollow microparticles and H-HAP/Au/PUA/PSS hybrid microparticles (B).

### 3.3 DOX loading and sustained release

H-HAP/Au/PUA/PSS hybrid microparticles with a hollow HAP core and polymer multilayer/AuNPs shell have the potential to be employed as the excellent drug vehicles with high drug loading efficiency and controllable release properties. Table 1 summarizes the drug loading efficiency of the samples. H-HAP/PUA/PSS and H-HAP/Au/PUA/PSS hybrid microparticles showed a relatively high drug loading efficiency

of around 60.0%, which was much higher than that of pure HAP microparticles (39.6%). It should be noted that the drug content is about 0.37 mg/10 mg for H-HAP/Au/PUA/PSS hybrid microparticles, which is a relatively high value for HAP based drug carriers.[8,17] It is clear that the inner hollow porous HAP core plays an important role in providing a strong adsorption for DOX molecules and then enhancing the drug loading efficiency of the hybrids. Moreover, the negatively charged PSS in the hybrid microparticles could provide additional attractive forces for the positively charged DOX due to the electrostatic interaction between PSS and DOX.[33] In addition, it must be noted that the AuNPs aggregates would potentially block drug molecules diffusing into the hollow microparticles during the drug loading process and then result in relatively low drug content. Therefore, the drug loading efficiency of H-HAP/Au/PUA/PSS hybrid microparticles (58.6%) is slightly lower than that of H-HAP/PUA/PSS hybrid microparticles (69.4%).

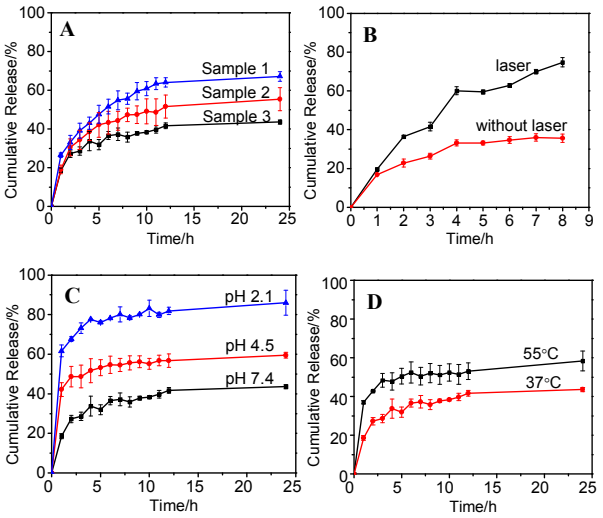


**Fig. 6.** DOX release profiles of HAP, H-HAP/PUA/PSS and H-HAP/Au/PUA/PSS hybrid microparticles at pH 7.4 and 37 °C (A), DOX release profiles of H-HAP/Au/PUA/PSS hybrid microparticles at pH 7.4, with or without the NIR laser irradiation (B), pH-dependent (C) and thermal-dependent release profiles (D) of H-HAP/Au/PUA/PSS hybrid microparticles.

The DOX release profiles of HAP microparticles, H-HAP/Au/PUA/PSS and H-HAP/PUA/PSS hybrid microparticles at 37 °C and pH 7.4 are showed in Fig. 6A. The DOX release from H-HAP/Au/PUA/PSS hybrid microparticles within 24 h was only 43%, whereas the value of HAP microparticles and H-HAP/PUA/PSS hybrid microparticles were 68% and 55%, respectively. The hollow interior serves as a drug reservoir, which could increase the drug loading efficiency and maintain a constant release rate. On the other hand, the polymer multilayer shell acts as a barrier to control the in-and-out of the drug. Polymer multilayer coating also avoid the direct contact between hollow HAP microparticles and the outside medium, which would reduce the drug release and assuage the initial burst release of DOX.[19] In addition, AuNPs aggregates inside hybrid particles would potentially decrease the permeability of the hybrid microparticles and then slow the DOX release.[31,35] A Student's t-test analysis was conducted to support this point; the *p* values between the release of H-HAP/Au/PUA/PSS and H-HAP/PUA/PSS hybrid microparticles, and the release of H-HAP/Au/PUA/PSS and HAP was 0.0275 and 0.0004, respectively. Both of the difference was statistically significant for the referred time period (greater than 95% confidence). Therefore, compared to solid HAP and H-HAP/PUA/PSS, H-HAP/Au/PUA/PSS hybrid microparticles show great potential as a novel drug carrier for sustained drug delivery.

### 3.4 NIR-responsive release

An important feature of AuNPs aggregates is NIR light-induced thermal effect, which could be employed for selective treatment of solid tumor.[23,24] To investigate the NIR-responsive release of DOX loaded H-HAP/Au/PUA/PSS hybrid microparticle, a CW diode laser with a centre wavelength of 780 nm was employed and the NIR-stimulus in vitro drug release behavior was performed in PBS solution with pH 7.4 (see Figure 6B). For sample without the NIR laser irradiation, only 32.5% DOX are released within 8 h. However, burst release was clearly observed upon NIR irradiation for 2 h. The cumulative release of DOX reached 74.7% within 8 h, which is significantly higher than that without NIR irradiation. The trigged rapid DOX release upon NIR irradiation is ascribed to the photothermal effect of AuNPs agglomerates within the polyelectrolyte multilayers absorbing the laser light energy,[36] which results in the partial collapse of PUA/PSS polyelectrlytes covering the exterior of the porous HAP as illustrated in Scheme 2.[37,38] Therefore, more DOX could release from the hollow hybrid HAP microparticles. Student's t-test analysis showed that the difference between the release of H-HAP/Au/PUA/PSS hybrid microparticles with and without laser was very statistically significant (*p* value was 0.0054, greater than 95% confidence).

### 3.5 pH-/thermal-sensitive release

Fig. 6C shows the pH-dependent release property of H-HAP/Au/PUA/PSS hybrid microparticles at 37 °C. It can be observe that the DOX release increased with decreasing pH from 7.4 to 2.1. Only 43.7% of DOX were released at pH 7.4 over 24 h, but almost 86.0% of DOX were released at pH 2.1 with the same treatment. Almost 70% of DOX were released at pH 2.1 within 2 h. Scheme 2 clearly indicated the structural changes of the hollow hybrid microparticles in acidic solution. The rapid release was partly due to the dissolution of HAP in the strong acidic solution.[39] In addition, with decreasing pH value, more and more amino groups of positive aliphatic PUA are protonated and the electrostatic repulsion between the positive charges results in a swelling structure. Therefore, the polyelectrolyte walls would gradually swell to facilitate the rapid release of DOX.[31,33] The *p* value obtained from Student's t-test analysis in the comparison between the release at pH 7.4 and 2.1 was less than 0.0001, the *p* value between the release at pH 7.4 and 4.5 were 0.0441. Both the difference was very statistically significant (greater than 95% confidence).

The LCST of aliphatic aliphatic PUA employed in the present study was around 50 °C. Therefore, we chose 37 °C, which were lower than the LCST, and 55 °C, which was higher than the LCST, as the temperature conditions in drug release study. Fig. 6D depicts the thermal-responsive release profiles of H-HAP/Au/PUA/PSS hybrid microparticles at pH 7.4. A temperature dependent response could be clearly observed, the

drug release at 55 °C was 15% higher than that at 37 °C. As illustrated in Scheme 2, when the temperature exceeded the LCST of PUA, polymer chains became shrunk and DOX molecules would be squeezed from the inside of the hybrid microparticles and the rapid DOX release would be observed.[9,11] The $p$ value between the release at 55 °C and 37 °C were less than 0.0001. The difference between these data was extremely statistically significant (greater than 95% confidence).

The in vitro drug release investigation demonstrated that the PUA/PSS polyelectrolyte multilayer and AuNPs agglomerates could not only reduce the drug release rate and assuage the initial burst release of DOX, but also endow the hybrid $CaCO_3$ microparticles with triple-responsive (NIR/pH/temperature) release properties. The studied hybrid microparticles can be used as novel "smart" vehicles for multi-responsive controlled drug delivery. As we known, NIR responsive matrix would increase the environmental temperature during the laser irradiation process.[32,40] Then, whether the elevated temperature derived from NIR irradiation would affect the thermal-responsive drug release property of the matrix? In the future, we will attempt to discover and discuss the relationship between the NIR-responsive property and thermal-responsive property of H-HAP/Au/PUA/PSS hybrid microparticles.

### 3.6 Drug Release Kinetics

The kinetics of DOX release from H-HAP/Au/PUA/PSS hybrid microparticles has been analyzed by plotting the cumulative release data versus time by fitting them to the following empirical equation:[19]

$$\frac{M_t}{M_\infty} = kt^n \qquad (1)$$

Here, $M_t$ is the cumulative amounts of DOX released at time $t$, and $M_\infty$ is the total amount of the microparticles, $k$ is a constant characteristic relating to the microparticles, and $n$ is the diffusion exponent characterizing the nature of the release mechanism. The DOX release kinetics of the samples at different conditions was analyzed and the values of $k$, $n$ and correlation coefficient ($R^2$) are shown in Table S1. Fig. S2A shows the curves of $\ln(M_t/M_\infty)$ versus $\ln t$ for H-HAP/Au/PUA/PSS hybrid microparticles at different pH values and temperatures. The $n$ values of the hybrids at pH 2.1 at 37 °C ranged from 0.977 to 0.116 and produced a shift from Case-II transport to Fickian diffusion.[41] This phenomenon may be attributed to the HAP dissolution and the corrosion of the PUA/PSS multilayers at pH 2.1. The $n$ values at pH 4.5 and pH 7.4 ranged from 0.815 to 0.133 and from 0.709 to 0.197, respectively, indicating a shift from anomalous transport to Fickian diffusion, which related to the polymer relaxation during polymer swelling. The n values at 55 °C and pH 7.4 were changed from 0.787 to 0.164, indicating that the DOX release was governed by the anomalous diffusion at the beginning of DOX release and the Fickian diffusion became dominant at the second stage.

Fig. S2B shows the curves of $\ln(M_t/M_\infty)$ versus $lnt$ for H-HAP/Au/PUA/PSS hybrid microparticles with and without NIR laser. The $n$ values of the hybrids with NIR laser ranged from 0.917 to 0.518 and produced a shift from Case-II transport to anomalous transport, which may be attributed to the polymer relaxation when AuNPs agglomerates changed light to heat during the laser irradiation. The n values of the hybrids without NIR laser ranged from 0.695 to 0.416, indicating a shift from anomalous transport to Fickian diffusion. Fig. S2C shows the curves of $\ln(M_t/M_\infty)$ versus $\ln t$ for HAP, H-HAP/PUA/PSS microparticles and H-HAP/Au/PUA/PSS microparticles at pH 7.4 and 37 °C. The $n$ value of HAP was 0.344, which was contributed to the unitary inorganic matrix without polymers. The $n$ values of H-HAP/PUA/PSS and H-HAP/Au/PUA/PSS hybrid microparticles ranged from 0.753 to 0.316 and from 0.709 to 0.197, respectively, indicating that the release changed from anomalous transport to Fickian diffusion. The results demonstrate that the introduction of PUA/PSS multilayer has obstructed the DOX diffusion and then changed the DOX release kinetics.

## 4. Conclusions

Hollow HAP/Au/PUA/PSS hybrid microparticles with a hollow HAP core and polymer multilayer/AuNPs shell for multi-responsive drug delivery have been prepared via LbL technique in the present paper. The AuNPs aggregates inside hybrid particles could potentially hinder DOX escaping from the hollow microparticles and assuage the initial burst release of DOX. More importantly, upon irradiation with NIR laser, AuNPs aggregates can effectively convert light to heat and result in the rapid release of DOX. In addition, the in vitro studies have clearly demonstrated the drug release of prepared hollow hybrid carriers exhibited distinguished pH- and thermal-dependent property. The present paper provides a facile and green route to fabricate smart hierarchical hybrid hollow drug carrier by combining polyelectrolytes, inorganic microparticles and metal nanoparticles, which is highly attractive for drug delivery area.

### Acknowledgements

This work was supported by grants from the National Natural Science Foundation of China (Projects 20874090 and 21074119).

### Notes and References

† *School of Materials Science and Engineering, Zhengzhou University, Zhengzhou 450052, China*

* *Correspondence author: Jun Shi or Shaokui Cao (E-mail: shijun@zzu.edu.cn, caoshaokui@zzu.edu.cn)*

† Electronic Supplementary Information (ESI) available: [Parameters $k$, $n$ and $R^2$ determined by Eq. (1) for the DOX release of samples at different release conditions, UV-vis light transmittance spectrum as a functional of temperature of aliphatic PUA solution, plots of $\ln(M_t/M_\infty)$ versus $\ln t$ for the release profiles of H-HAP/Au/PUA/PSS hybrid microparticles at different pH values and temperatures].

1 J. Zhang, X. D. Xu, Y. Liu, C. W. Liu, X. H. Chen, C. Li, R. X. Zhuo, X. Z. Zhang, *Adv. Funct. Mater.* 2012, **22**, 1704.
2 F. Wang, Y. Zhu, C. Y. Gao, *Colloids Surf., A* 2009, **349**, 55.
3 Q. H. Zhao, B. Y. Li, *Nanomed.: Nanotechnol.* 2008, **4**, 302
4 V. Lapeyre, N. Renaudie, J. F. Dechezelles, H. Saadaoui, S. Ravaine, V. Ravaine, *Langmuir* 2009, **25**, 4659.
5 Y. Jiang, F. Zeng, R. Y. Gong, Z. X. Guo, C. F. Chen, X. B. Wan, *Soft Matter* 2013, **9**, 7538-7544.
6 Q. C. Yuan, O. J. Cayre, S. Fujii, S. P. Armes, R. A. Williams, S. Biggs, *Langmuir* 2010, **16**, 18408.
7 S. Berger, H. P. Zhang, A. Pich, *Adv. Funct. Mater.* 2009, **19**, 554.
8 X. H. Wang, G. H. Jiang, X. Li, B. L. Tang, Z. Wei, C. Y. Mai, *Polym. Chem.* 2013, **4**, 4574-4577.
9 H. Wu, J. Dong, C. C. Li, Y. B. Liu, N. Feng, L. P. Xu, X. W. Zhan, H. Yang, G. J. Wang, *Chem. Commun.* 2013, **49**, 3516-3518.

10 R. M. Yang, S. H. Peng and T. C. Hughes, Soft Matter, 2014, **10**, 2188-2196.
11 S. C. Tang, Z. Q. Shi, Y. Cao and W. He, *J. Mater. Chem. B*, 2013, **1**, 1628–1634.
12 S. D. Jiang, Q. Z. Yao, G. T. Zhou and S. Q. Fu, *J. Phys. Chem. C*, 2012, **116**, 4484–4492.
13 K. Watanabea, Y. Nishiob, R. Makiurac, A. Nakahirab and C. Kojimac, *Int. J. Pharm.*, 2013, **446**, 81–86.
14 F. F. Li, Y. Liu, Y. Ding, Q. F. Xie, *Soft Matter* 2014, **10**, 2292-2303.
15 M. Y. Ma, Y. J. Zhu, L. Li and S. W. Cao, *J. Mater. Chem.*, 2008, **18**, 2722–2727.
16 Y. H. Yang, C. H. Liu, Y. H. Liang, F. H. Lin and K. C. W. Wu, *J. Mater. Chem. B*, 2013, **1**, 2447–2450.
17 F. Ye, H. F. Guo, H. J. Zhang and X. L. He, Acta Biomater., 2010, **6**, 2212–2218.
18 Y. S. Wang, M. S. Hassan, P. Gunawan, R. Lau, X. Wang and R. Xu, *J. Colloid Interface Sci.*, 2009, **339**, 69–77.
19 D. S. Feng, J. Shi, X. J. Wang, L. Zhang and S. K. Cao, *RSC Adv.*, 2013, **3**, 24975-24982.
20 M. Delcea, N. Sternberg, A. M. Yashchenok, R. Georgieva, H. Bäumler, H. Möhwald, A. G. Skirtach, *ACS Nano*, 2012, **6**, 4169-4180.
21 A. G. Skirtach, C. Dejugnat, D. Braun, A. S. Susha, A. L. Rogach, W. J. Parak, H. Möhwald, G. B. Sukhorukov, *Nano Lett.* 2005, **5**, 1371-1377.
22 S. Carregal-Romero, M. Ochs, P. Rivera-Gil, C. Ganas, A. M. Pavlov, G. B. Sukhorukov, W. J. Parak, *J. Controlled Release*, 2011, **159**, 120–127.
23 C. R. Susana, M. Ochs, R. G. Pilar, G. Carolin , *J. Controlled Release*, 2012, **159**, 120-127.
24 M. F. Bedard, D. Braun, *ACS Nano*, 2008, **2**, 1807-1816.
25 X. H. Ji, X. N. Song, J. Li, B. Y. Bai, W. S. Yang and X. G. Peng, *J. Am. Chem. Soc*, 2007, **129**, 13939-13948
26 O. Ihata, Y. Kayaki, T. Ikariya, *Chem. Commun.* 2005, **17**, 2268.
27 O. Ihata, Y. Kayaki, T. Ikariya, *Macromolecules* 2005, **38**, 6429.
28 J. Shi, J. Shi, C. Du, Q. Chen and S. K. Cao, *J. Membr. Sci.*, 2013, **433**, 39–48.
29 L. Gu, X. H. Wang, X. S. Chen, X. J. Zhao, F. S. Wang, *J. Polym. Sci., A* 2011, **49**, 5162.
30 M. Yang, R. Alvarez-Puebla, H.-S. Kim, P. Aldeanueva-Potel, L. M. Liz- Marzan, N. A. Kotov, *Nano Lett.* 2010, **10**, 4013.
31 C. Du, J. Shi, J. Shi, L. Zhang and S. K. Cao, *Mater. Sci. Eng. C*, 2012, **33**, 3745-3752.
32 R. Kurapati, A. M. Raichur, *Chem. Commun.* 2013, **49**, 734-736.
33 J. Shi, C. Du, J. Shi, Y. Wang and S. K. Cao, *Macromol. Biosci.*, 2013, **13**, 494–502.
34 V. Kozlovskaya, E. Kharlampieva, I. Drachuk, D. Cheng and V. V. Tsukruk, *Soft Matter* 2010, **6**, 3596-3608.
35 J. Shi, Z. Z. Zhang, G. F. Li and S. K. Cao, *J. Mater. Chem.*, 2011, **21**, 16028–16034.
36 A. M. El-Toni, F. Zhang, D. Y. Zhao, *Chem. Mater.*, 2013, **25**, 3030–3037.
37 B. Hu, L. P. Zhang, X. W. Chen, J.H. Wang, *Nanoscale*, 2013, **5**, 246-252.
38 A. S. Angelatos, B. Radt, F. Caruso, *J. Phys. Chem. B*, 2005, **109**, 3071-3076
39 J. Shi, W. Y. Qi, G. F. Li and S. K. Cao, *Mater. Sci. Eng. C*, 2012, **32**, 1299-1306.
40 S. Shen, H. Y. Tang, X. T. Zhang, J. F. Ren, Z. Q. Pang, D. G. Wang, H. L. Gao, Y. Qian, X. G. Jiang, W. L. Yang, *Biomaterials*, 2013, **34**, 3150-3158.
41 P. L. Ritger and N. A. Peppas, *J. Controlled Release*, 1987, **5**, 37-42.




 